

Original Article



Transcriptional modulation of skin cells using liganded immodulin peptides

Desmond D. Mascarenhas^{1,2*}, Bhaumik Patel³, Puja Ravikumar³, Edward Amento³, Ajay Bhargava⁴

¹ Mayflower Research Institute; Sunnyvale, CA 94085, USA

² Transporin Inc, Sunnyvale, USA

³ Molecular Medicine Research Institute, Sunnyvale, CA, USA

⁴ Shakti Bioresearch LLC, Watertown, USA

Article Info

Abstract



Article history:

Received: January 06, 2025

Accepted: February 28, 2025

Published: March 31, 2025

Use your device to scan and read the article online



Immodulins are synthetic peptides that efficiently utilize iron-mediated cellular uptake, importin-mediated nuclear translocation and binding to retinoid X receptor to mediate transcriptional effects. The possible use of side-chain derivatized immodulins (SCDI) as tunable therapeutic agents is explored in this work. Biodistribution studies show that, when applied transdermally to rats using a nanoemulsion, immodulin peptides rapidly partition to skin tissue resulting in a 9X enrichment in skin relative to plasma, even at skin locations distant from the site of application. We show that optimized side-chain derivatization of immodulins with selected ligands of RXR heterodimeric partners can stimulate by one to three orders of magnitude: [a] CD169+CCL22+ macrophage differentiation (RAR α / β ligand); [b] IL-19, IL-22 and IL-24 production by HaCaT keratinocytes (RAR γ agonist); and [c] FGF7/KGF-1, TGF β and COL1A1 by dermal fibroblasts (partial PPAR γ ligand); all $p < 0.01$. Differentiated CD169+ macrophages, in turn, drive the conversion of FoxP3 CD4+ Tcells into iTregs (>4 -fold, $p < 0.01$) while reducing IL-17 levels >4 -fold ($p < 0.01$). In addition, myoblast differentiation is stimulated $>10X$ by a PPAR α ligand ($p < 0.01$). These processes resemble key features of paracrine circuitry in skin known to be involved in wound healing. Versatile SCDI scaffolds hold promise for the rapid and inexpensive development of safe, targeted, self-administered therapeutic agents for skin.

Keywords: Immodulin, Peptide, Ligand, Anatomical targeting, Therapeutic, Transcription.

1. Introduction

In order to mitigate development costs, new drug design may attempt to triangulate the evolution of healthcare delivery systems, regulatory agencies' growing emphasis on safety, patent life considerations and emerging consumer preferences regarding treatment modalities. Such cross-currents saddle drug designers with the need to devise novel approaches. Historically, small-molecule drugs have been administered as pills or injectables in doses that are sufficient to flood the body. As a rule, these molecules lack guidance systems for precisely finding the anatomic locations that require their therapeutic action, leading to a plethora of off-target side effects. One possible conceptual approach to this problem is to marry the diversity achievable by combining old, clinically vetted chemical entities with the evolved biological "intelligence" of natural molecules [1-3].

So far, drug-targeting technologies have mainly homed to cell-surface targets, an approach of limited value for epigenetic drugs such as HDAC inhibitors and nuclear receptor ligands. In this study, we explore the use of small chemical molecules with known epigenetic bioactivity as

side chains of immodulin peptides [1]. Immodulins are synthetic equivalents of natural protein sequences from a family of insulin-like growth factor binding proteins that direct the modulation of retinoid X receptor (RXR) — a master transcriptional regulator. Immodulins are capable of cell targeting, iron-mediated cell entry, nuclear translocation and direct binding to RXR [1,2]. As such, they offer a scaffold for efficient linkage and delivery of small-molecule epigenetic modulators to a precisely identified transcriptional complex inside the cell nucleus of any mammalian cell. Hundreds of RXR-heterodimer-specific small-molecule modulators have been investigated, including PPAR and RAR ligands [3-8]. Some, such as fenofibrate, tamibarotene and palovarotene have gained regulatory approval as drugs in their own right, despite their inherent targeting inefficiencies *in vivo* [9].

Emerging patient demands [10], have resulted in elevated compound average growth rates for products and services suited to "distance medicine". These trends point to self-administered drug modalities such as transdermals, inhalants and nasal sprays. An unspoken requirement of such market evolution towards unsupervised patient drug

* Corresponding author.

E-mail address: desmond@transporin.com (D. Mascarenhas).

Doi: <http://dx.doi.org/10.14715/cmb/2025.71.3.15>

use is the need for broader therapeutic indexes. In theory, the SCDIs explored in this study could align well with future therapeutic contexts if sufficient anatomical and mechanistic precision could be demonstrated. In this study, we use the biodistribution of immodulins in rats to demonstrate their surprising homing to skin tissue, and cultured skin cells to demonstrate the mechanistic specificity of SCDIs in major cell types found within the targeted tissue.

2. Materials and Methods

2.1. Peptide synthesis and chemical reagents

All peptides used in this study were synthesized by Lifetein LLC (Hillsborough, NJ) and purified to >80% purity. Identity was confirmed by mass spectroscopy. The THP1-Dual monocyte reporter cell line was purchased from Invivogen Inc., San Diego, CA. HaCaT cells were from AddexBio (Cat No. T0020001, Lot No. 0003798). The C2C12 myoblast cell line and HFF-1 human dermal fibroblasts (Cat No. SCRC-1041, Lot No. 64287435) were obtained from the American Type Culture Collection (ATCC, Manassas, VA). Normal Human Peripheral CD+ Naïve T Cells were from ZenBio (Cat No. SER-CD4+NT, Lot No. CD4TN012714A). Unless otherwise specified, chemical reagents were purchased from Cayman Chemical Company (Ann Arbor, MI), Medchem Express (Monmouth Junction, NJ) or Sigma-Aldrich Chemical Compa-

ny (St. Louis, MO).

2.2. N-terminal modification of peptide with carboxylic acids of low molecular mass.

N-terminal modification of peptides with biotin, or fatty acids such as myristic and palmitic acids, has been widely instantiated, but this type of modification using other kinds of carboxylic acids is rarely reported. Coupling of small molecules to one or both of two substrates, immodulin peptide *imm3* or a generic D-tetrapeptide dLys-dAsp-dLys-dPro was performed. Similar efficiencies of coupling were observed for either peptide, thereby demonstrating the generality of the method. However, only a minority of the compounds gave sufficiently high yields of correct product. Peptides were synthesized according to a common Fmoc/tBu solid phase synthesis strategy. Synthesis was done manually or automated, with similar results. After the peptide synthesis, the resin was divided into batches of 20 μ mol. Each batch was treated with one of the organic compounds specified in Table 1. The coupling was carried out using 2 equivalents of the compound, 2.4 equivalents of activator HATU or HCTU, and 4 equivalents of NMM base. The reaction mixture was renewed after 2 hrs reaction time and allowed to react another 4 hrs or overnight. After washing the resin several times with dimethylformamide (DMF), and subsequently with dichloromethane

Table 1. N-terminal modification of peptide with non-amino acid carboxylic acids of low molecular mass.

<i>Compound</i>	<i>CAS No.</i>	<i>MW</i>	<i>Yield T4*</i>	<i>Yield IM3*</i>
oleic acid	112-80-1	282.5	44.21%	
eicosapentaenoic acid	10417-94-4	302.5	66.79%	
lignoceric acid	557-59-5	368.6	89.20%	
capric acid	1002-62-6	172.2	88.67%	98.0%
docosahexanoic acid	6217-54-5	368.6	57.77%	
lauric acid	143-07-7	200.3	85.14%	96.7%
10-hydroxy-2-decenoic acid	14113-05-4	186.3	44.38%	
ferulic acid	1135-24-6	194.2	26.58%	
isoferulic acid	537-73-5	194.2	55.80%	70.2%
Aspirin	50-78-2	180.2	56.5%	
valeroyl salicylate	64206-54-8	222.2	11.76%	
betulinic acid	472-15-1	456.7	<1%	
Rhein	478-43-3	284.2	50.95%	
Diacerein	13939-02-1	368.3	43.2%	
2,7-dichlorodihydro- fluorescein diacetate	4091-99-0	487.3	91.2%	
(s)-ketoprofen	22161-81-5	254.3	77.86%	
Ibuprofen	15687-27-1	206.3	93.42%	98.0%
trans-cinnamic acid	140-10-3	148.2	93.12%	81.5%
(s)-(-)-perillic acid	23635-14-5	166.2	27.96%	
fenofibric acid	42017-89-0	318.8	85.67%	99.9%
Indomethacin	53-86-1	357.8	87.5%	85.2%#
valproic acid	1069-66-5	144.2	91.43%	84.9%
2-hexyl-pentynoic acid	96017-59-3	182.3		85.1%
RG-108	48208-26-0	334.3		74.3%@
all-trans retinoic acid	302-79-4	300.4	13.1%	
Bexarotene	153559-49-0	348.5	97.09%	94.4%

*Percent yield of correct species by mass spectroscopy for T4 (tetrapeptide) and IMM3 immodulin peptide substrates. Yields >80% are shown in bold type; # lost p-chlorophenone group (incorrect product); @ indole core oxidized by Arg protecting groups (incorrect product). See Methods for coupling procedure.

(DCM), the batches were dried. For peptide cleavage, the resins were treated with 1% dithiothreitol (DTT), 2% water and 3% TIPS in trifluoroacetic acid (TFA) for 3.5 hrs. The cleavage solution was separated from the resin and treated with diethylether/n-pentane (1:1). The resulting precipitate was centrifuged and the pellet was washed three times in the same DEE/pentane mixture. The recovered peptide was air-dried and stored at -20 degrees C or further purified by high-performance liquid chromatography (HPLC) using a 0-50% acetonitrile gradient, 0.1% TFA (20 min).

2.3. Carboxyterminal lysine side-chain derivatization with nuclear receptor ligands

The peptides were synthesized on ChemMatrix Rink Amide resin using a modified Fmoc synthesis protocol with DIC/Cl-HOBt coupling on an APEX 396 automatic synthesizer. For example, using X to represent the small-molecule carboxylate nuclear receptor ligand compound to be covalently bound to the epsilon amine of the carboxyterminal lysine, Fmoc-d-Lys(X)-OH was customized as follows: compound X was activated as an NHS-ester and then reacted with the free epsilon amine side chain of Fmoc-d-Lys-OH. Fmoc-d-Lys(X) resin was then swollen in DMF for 30 min, treated with 20v% Piperidine-DMF for 8 minutes to remove the Fmoc protecting group at 50°C, and washed with DMF three times. For the coupling reaction, the resin was added with Fmoc-protected amino acid, Cl-HOBt, DIC and N-Methyl-2-pyrrolidone (NMP). The mixture was vortexed for 20 minutes at 50°C. Afterwards, the resin was washed with DMF once. The cycle of deprotection and coupling steps was repeated until the last residue in the sequence had been added. The resin was then washed with DMF, DCM and dried with air. The peptide was cleaved from the resin using a TFA cocktail (95v%TFA, 2.5v%water and 2.5v%TIS) for three hours. Crude peptides were precipitated in ice-chilled anhydrous ethyl ether and washed three times with ethyl ether before being dried in vacuo. The purification was performed by preparative HPLC. The results of the conjugation experiments show that there is wide variation in conjugation efficiency from compound to compound. Once shown successfully, however, the C-terminal modification of an immodulin peptide with a given compound is highly reproducible. Some examples are shown in Table 2.

2.4. Preparation of nanoemulsion and PLGA microparticles

NENP nanoemulsion was 6 mM sodium acetate buffer pH 5.2, 16% glycerol, 16% PEG-400, 12% carbitol, 4% propylene glycol, 2% Tween-80, 10 mM levulinic acid, 5 mM menthol, 5 mM p-anisic acid, 5 mM verbenone, 1 mM linalool, 1 mM ferulic acid and 1 mM glycyrrhizic acid. COOH-capped poly(D, L-lactide-co-glycolide), LA/GA 50:50, MW-10K (PLGA) was purchased from Nanosoft Polymers (Winston-Salem, NC). PLGA-M was 50 mg/ml PLGA, 4.25 mg/ml L-menthol in acetone. The 125 uL peptide mix contained 100 ug imm3SVD peptide and 100 µg of Alexa488- or horseradish-peroxidase-labelled-streptavidin (AAT BioQuest, Pleasanton, CA) in saline buffer. For the transferrin release experiment, 800 ug recombinant human holotransferrin was also added. 80 uL of this peptide mix was mixed with 1.0 ml PLGA-M with rapid vortexing. 2 ml of polyvinyl alcohol was added, and the mixture was vortexed again, added to an open 50 ml tube containing 20 ml sterile distilled water and shaken at room temperature for at least 4 hours. Microparticles were harvested by centrifugation (Beckman table-top, 4,000 rpm, 10 minutes), washed in 1 ml sterile distilled water (3X), then serially coated by suspension in 0.5 ml of a saturated solution of glycol-chitosan (Santa Cruz Biotech, CA) and 0.5 ml of 20 mg/ml human serum albumin (Sigma) for 30 minutes at room temperature. This step was followed by washing (2X) and resuspension of microparticles in 0.4 ml sterile distilled water. PLGA microparticle preparations were stored at -20 degrees C.

2.5. Biodistribution studies in rats, and scald-endotoxemia model

All animal procedures were performed in adherence with the National Institute of Health's Guide for Care and Use of Laboratory Animals and approved by the Institutional Animal Care and Use Committee (IACUC). The animal study protocol was approved by the Institutional Review Board of the Molecular Medicine Research Institute. All animal studies complied with the NIH Guide for the Care and Use of Laboratory Animals. Adult male Sprague Dawley rats (250–300 gm, Charles River Laboratories, Wilmington, MA, USA) were used in this experiment. 4-8 animals per group (as shown in Table 3) were housed with access to food and water ad libitum. The

Table 2. Nuclear receptor (NR) ligands used for lysine side chain derivatization.

NR Ligand	Compound	CAS No.	MW
PPAR α	2-[[4-[2-[[[(cyclohexylamino)carbonyl](4-cyclohexylbutyl)amino]ethyl]phenyl]thio]-2-methyl-propanoic acid	265129-71-3	502.8
PPAR γ	Capric acid (decanoate)	1002-62-6	194.2
PPAR $\alpha\beta\gamma$	2-[4-(4-chlorobenzoyl)phenoxy]-2-methyl-propanoic acid	42017-89-0	318.8
FXR	3-[2-[2-chloro-4-[[3-(2,6-dichlorophenyl)-5-(1-methylethyl)-4-isoxazolyl]methoxy]phenyl]ethenyl]-benzoic acid	278779-30-9	542.8
RAR $\beta\gamma$	6-(4-methoxy-3-tricyclo[3.3.1.1 ^{3,7}]dec-1-ylphenyl)-2-naphthalenecarboxylic acid	106685-40-9	412.5
RAR $\alpha\beta$	4-[[[(5,6,7,8-tetrahydro-5,5,8,8-tetramethyl-2-naphthalenyl)amino]carbonyl]-benzoic acid	94497-51-5	351.4
RAR α	4-[[[(5,6,7,8-tetrahydro-5,5,8,8-tetramethyl-2-naphthalenyl)carbonyl]amino]-benzoic acid	102121-60-8	351.4
RAR γ	4-[(1E)-2-[5,6,7,8-tetrahydro-5,5,8,8-tetramethyl-3-(1H-pyrazol-1-ylmethyl)-2-naphthalenyl]ethenyl]-benzoic acid	410528-02-8	414.5
RXR	4-[1-(5,6,7,8-tetrahydro-3,5,5,8,8-pentamethyl-2-naphthalenyl)ethenyl]-benzoic acid	153559-49-0	348.5

See the Methods section for details of side-chain derivatization procedure.

Table 3. Tissue label per mg protein at 2 hours post-administration (expressed as a multiple of plasma concentration).

PLASMA CONTROL	1.00 ± 0.35	1.00 ± 0.05	1.05 ± 0.00	1.00 ± 0.23	1.00 ± 0.07
GP1: FORELIMB SKIN	4.30 ± 0.86	5.36 ± 1.22	2.07 ± 0.57	11.11 ± 1.58	14.69 ± 6.42
GP1: CALF SKIN	3.95 ± 0.76	3.31 ± 1.13	2.97 ± 1.54	9.23 ± 2.98	8.48 ± 5.98
GP1: BRACHIAL LN	3.29 ± 0.46	4.01 ± 0.45	3.65 ± 0.42	12.32 ± 1.99	7.05 ± 1.17
GP1: POPLITEAL LN	3.61 ± 1.32	4.46 ± 0.96	3.64 ± 0.72	8.59 ± 0.76	10.27 ± 1.90
GROUP 1 AVERAGE	3.79 ± 0.44	4.28 ± 0.86	3.08 ± 0.75	10.31 ± 1.71	10.12 ± 3.32
GP2: SM. INTESTINE	6.06 ± 0.93	5.48 ± 1.44	6.43 ± 1.75	3.83 ± 0.21	1.80 ± 0.79
GP2: KIDNEY	7.47 ± 0.76	13.15 ± 0.72	15.00 ± 0.27	2.82 ± 0.19	4.33 ± 0.40
GP2: HEART	7.25 ± 0.61	6.03 ± 0.83	9.71 ± 0.71	6.85 ± 0.22	2.22 ± 0.37
GP2: LIVER	7.91 ± 0.74	9.01 ± 0.15	12.36 ± 0.13	4.47 ± 0.66	4.20 ± 0.07
GP2: PANCREAS	4.67 ± 1.12	3.26 ± 0.07	4.02 ± 0.21	3.07 ± 0.61	1.59 ± 0.06
GROUP 2 AVERAGE	6.67 ± 1.31**	7.39 ± 3.82 (NS)	9.50 ± 4.42*	4.21 ± 1.61**	2.83 ± 1.33*
GP3: BICEPS	nd	2.63 ± 0.91	2.65 ± 1.25	nd	1.33 ± 0.37
GP3: TRICEPS	1.25 ± 0.21	2.94 ± 1.26	2.87 ± 2.16	2.02 ± 0.82	1.17 ± 0.58
GP3: EDL	1.68 ± 0.54	3.43 ± 1.79	3.40 ± 2.53	2.85 ± 0.64	1.39 ± 0.09
GP3: SOLEUS	2.58 ± 0.52	2.34 ± 1.07	1.56 ± 0.79	3.02 ± 0.26	1.49 ± 0.69
GP3: FLEXOR ULNARIS	1.82 ± 0.57	nd	nd	2.53 ± 0.53	nd
GROUP 3 AVERAGE	1.83 ± 0.55**	2.83 ± 0.46*	2.62 ± 0.77 (NS)	2.61 ± 0.44**	1.34 ± 0.13*
GP4: INGUINAL LN	3.09 ± 0.31	4.53 ± 0.66	4.32 ± 0.42	7.08 ± 2.07	5.45 ± 1.37
GP4: MESENTERIC LN	6.48 ± 0.77	5.85 ± 0.82	7.26 ± 0.47	2.52 ± 0.59	2.75 ± 1.00
GP4: SPLEEN	1.72 ± 0.19	2.26 ± 0.06	2.16 ± 0.12	6.40 ± 0.63	2.22 ± 0.20
GROUP 4 AVERAGE	3.76 ± 2.45 (NS)	4.21 ± 1.82 (NS)	4.58 ± 2.56 (NS)	5.33 ± 2.46*	3.48 ± 1.73*
CNS (Olfac. Lobe)	1.46 ± 0.12	2.80 ± 0.12	2.88 ± 0.23	nd	1.47 ± 0.08
LUNG	2.13 ± 0.16	3.34 ± 0.59	2.59 ± 0.26	7.11 ± 0.53	2.72 ± 1.18

nd = not determined; * p<0.05, ** p<0.01 versus Group 1 average; NS= not significant; IN=intranasal, SQ=subcutaneous injection; TD-f=transdermal (forearm); TD-c=transdermal (calf); Label [A] = SA488; Label [B] = SA-HRP.

forelimbs and/or hindlimbs and the back of the rat were shaved a day before the experiment. This, and all other study procedures, including transdermal treatments and subcutaneous injections, were performed under general anesthesia using isoflurane. At the end of the study period, animals were euthanized by carbon dioxide as approved by IACUC guidelines, the NIH's Office of Laboratory Animal Welfare (OLAW), and AVMA recommendations. All tissues and organs of interest were rapidly dissected or collected and flash-frozen in liquid nitrogen for subsequent storage at -80 °C. For endotoxemia experiments, adult male Sprague Dawley rats (group n=6) were treated and analyzed as previously described [16]. Briefly, after the 7-day peptide dosing period (i.e. on day 8), scald group animals received a single subcutaneous bolus injection of 0.5 mg/kg LPS (Sigma Chemical Co., St. Louis, MO). For each animal, pulse rate (bpm) and breathing distension (um) were monitored by oximetry (MouseOx Oximeter, STARR Life Sciences, Oakmont, PA). Oximeter readings were standardized and expressed as a percentage based on each animal's basal values measured just prior to the start of the experiment. Breathing difficulty was expressed as the product of pulse rate (bpm) and breathing distension (um). Under optimal anesthesia, the heart rate is kept between 300 bpm and 450 bpm, with oxygen saturation at 97%–98%.

2.6. Cell culture

The C2C12 myoblast cell line was cultured in DMEM medium supplemented with 10% fetal bovine serum (FBS) and 1% penicillin/streptomycin. For differentia-

tion, cells were cultured in the same medium, except that 10% FBS was replaced by 2% horse serum. Peptides and inhibitors were added at the indicated concentrations and cells were harvested 96 hours later for assay. Cell extracts were assayed for creatine kinase (CK) per mg protein. CK was measured using the ECPK-100 kit from BioAssay Systems (Hayward, CA). Protein was assayed using the BCA protein assay kit from Thermofisher Scientific (Waltham, MA). Macrophage differentiation and polarization assays were done using the THP1-Dual monocyte reporter cell line, which was seeded at 3x10⁴ cells per well in 96-well plates and cultured at 37 degrees C in RPMI-1640 growth medium plus 10% fetal bovine serum and 1% penicillin/streptomycin, then treated for 24 hours with 100 ng/ml phorbol-12-myristate-13-acetate. Peptide (330 or 660 nM) was added, and the incubation continued for an additional 24 hours. Culture supernatants were assayed for CCL22, IL-10 or TGFβ using DuoSet ELISA kits (R&D Systems, Minneapolis, MN). Adherent cells were washed twice with PBS and cells were assayed for immunoreactivity of surface marker CD169 using biotin-labeled anti-human CD169 antibody purchased from Miltenyi Biotec (Auburn, CA) and a streptavidin-horseradish peroxidase/TMB secondary detection reagent. Results were expressed as arbitrary ELISA immunoreactivity units relative to the control peptide set to =100. For T-cell overlay experiments, PMA-treated THP1-Dual cells were first cultured and treated with peptide for 24 hours as described above. Naïve, 1X10⁶ T-cells were thawed in 5 mL of RPMI-1640 medium, centrifuged and resuspended in 5 mL of the same medium containing penicillin/streptomycin. 100 μL

of T-cells were layered on each THP1-Dual culture well along with 10 μ L of test peptide (330-660 nM) and 10 μ L of activation beads (Dynabeads™ Human T-Activator CD3/CD28 for T Cell Expansion and Activation, Cat. No. 11161D, Thermofisher Scientific, Santa Clara, CA), then incubated in a humidified incubator at 37 °C with 5% CO₂ for 96 hours. Supernatants were assayed for cytokines as above. Cell extracts were assayed for total protein and for FoxP3 by ELISA. HFF-1 and HaCaT cell lines were cultured in DMEM medium supplemented with 10% fetal bovine serum (FBS) and 1% penicillin/streptomycin. HFF-1 (1250 cells/well) or HaCaT (2500 cells/well) were plated in 96-well plates and incubated in a humidified incubator at 37 °C with 5% CO₂. After overnight incubation, peptides were added at indicated concentrations in 4 wells each. For IL-19, IL-22 and IL-24 assays, HaCaT cell culture additionally included 10 ng/ml TNF α and 100 ng/ml IFN γ . After 24 hours of incubation, supernatants were harvested and assayed for IL-19, IL-22 and IL-24 (HaCaT), TGF β -1 or KGF-1 (HFF-1) by ELISA. The cells were rinsed with fresh medium, 100 μ L of fresh medium and 100 μ L of CTG assay reagent (Promega, Madison, WI) was added. After 10 minutes plates were read in a GloMax luminescence reader. This confirmation of full cell viability was used to ensure that none of the treatments were toxic to cells. All cell culture data were collected in quadruplicate, and the reported observations were representative of at least two independent experiments.

2.7. Statistical analysis

Data are presented as means \pm standard deviation (SD) unless otherwise indicated. Probability values (*p*-values) were computed using Student's *t*-test and expressed relative to control treatment, as indicated.

3. Results

3.1. Pharmacokinetics

We formulated fluorescently-labelled immodulin peptides in PLGA microparticles for rat pharmacokinetic studies, as described in Methods. We compared naked peptides with PLGA-wrapped peptide microparticles by administering to rats via subcutaneous bolus injection. In addition, we also administered the PLGA formulation via the intranasal route.

The results are shown in Figure 1A, which shows a 5-10X increase in area under the curve (AUC) for the peptide-PLGA microparticles compared to naked peptide when administered via subcutaneous bolus injection. There was no significant difference in AUC between peptide-PLGA when administered by subcutaneous bolus versus the intranasal route, though release kinetics seemed slightly delayed in the latter case. Accumulation of label in tissues was consistent with these results (not shown): PLGA-wrapped peptide showed 5-10X higher levels in tissue compared to naked peptide, as a percentage of input counts, regardless of whether the route of administration was subcutaneous bolus injection or intranasal application. We therefore proceeded with peptide-PLGA microparticle formulations for our biodistribution studies.

3.2. Biodistribution in rats

The relative biodistribution of PLGA microparticle-formulated immodulin peptide at 120 minutes post-administration is shown in Table 3. Studies using SA488

fluorescent label and SA-HRP enzymatic label gave very similar biodistribution results via subcutaneous bolus. Biodistribution using intranasal or subcutaneous routes is similar, but transdermal administration of the same PLGA-peptide formulation shows a striking 9-fold higher relative partitioning of label to skin and skin-draining lymph nodes when compared to plasma and major abdominal organs, where serious drug toxicities are most often registered. Since the biodistribution to the skin of upper and lower limbs was similar, regardless of *whether the PLGA-peptide formulation was applied transdermally to the calf or to the forearm*, the peripheral tissue enrichment observed does not seem to be simply a local phenomenon at the site of application but an active partitioning of the peptide to surface lymphatics, consistent with the low levels seen in plasma. By contrast, accumulation of peptides in the mesenteric lymph nodes of these animals is lower. To our knowledge, there are no prior examples of comparable skin tissue enrichment at remote sites, regardless of the site of application. The implications of these distribution data for the therapeutic index of a drug candidate are potentially significant. Figure 1B shows how this unexpected biodistribution affects the relative exposure to peptide for several major abdominal organs when compared to skin and skin-draining lymphatics. Such anatomical specificity bears upon the possible use of immodulin peptides as scaffolds for designing therapeutics to treat dysfunctions of the skin or the peripheral immune system.

3.3. Construction of derivatized immodulins

We next investigated the possibility of derivatization at (a) the N-terminus and/or (b) at a carboxyterminal lysine (epsilon amino) side-chain of an immodulin peptide. Our goal was to show that a small-molecule carboxylate of choice can be attached at either or both of these locations via an amide bond. If the process is to be industrially scalable, integration of these steps with automated chemical synthesis of the peptide is desirable. Modern Fmoc-based peptide synthesis proceeds from the C-terminus toward the N-terminus. The chemistry of covalent attachment of a small non-amino acid molecule at either end of the peptide thus faces very different challenges. If an unprotected lysine epsilon amino group is to be used for covalent attachment of a non-amino acid carboxylate on or near

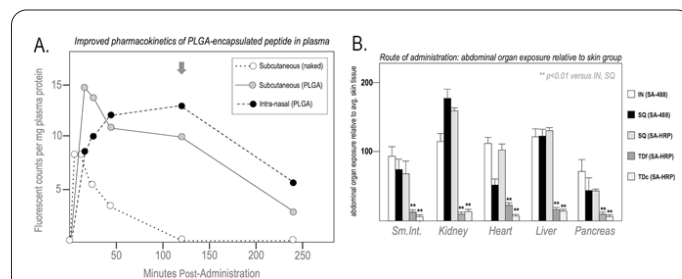


Fig. 1. Pharmacokinetics of immodulin peptide and tissue exposure in rats. (A) Plasma samples were taken at the indicated time-points after administration of fluorescent-labelled naked or PLGA-microsphere-encapsulated imm3SVD peptide. The arrow indicates the timepoint selected for biodistribution studies. (B) Relative biodistribution (fluorescent counts or enzymatic units per mg tissue protein) of peptide to major abdominal organs compared to skin tissues, compared by route of administration (type of label used in parentheses). IN=intranasal, SQ=subcutaneous bolus, Tdf= transdermal/forearm, Tdc=transdermal/calf. ** *p*<0.01 versus IN and SQ.

the C-terminus, that compound must be stable enough to survive subsequent cycles of elongation under the harsh conditions of modern automated peptide synthesis. On the N-terminus, by contrast, issues of cost are paramount in selecting a compound for attachment because, for a peptide longer than, say, thirty residues, the mix would predictably contain a large fraction of failure sequences that typically accumulate during longer chain elongation, necessitating a sufficient excess of compound for the reaction. Thus, cost at scale can become prohibitive for some compounds.

Table 2 shows the results obtained when a variety of relatively inexpensive compounds were used for covalent attachment at the N-terminus of two different peptides: a model tetramer and an immodulin 22-mer (peptide *imm3*, Table 4). The results show that only a fraction of the compounds generated the predicted product efficiently enough to be useful at industrial scale (we employed an arbitrary cutoff of >80%). Those that could be covalently attached successfully, did so reproducibly. Thus, compounds vary greatly in their suitability for covalent attachment, for reasons that are as yet unclear. Advance inspection of the molecular structures by experienced chemists did not generate accurate predictions of success. Likewise, Table 2 shows cases of nuclear receptor (NR) ligands such as bexarotene (RXR), GW7647 (PPAR α), decanoic acid (PPAR γ), tamibarotene (RAR α/β) and palovarotene (RAR γ) that were successfully coupled to the C-terminal lysine of an immodulin peptide. The majority of NR ligand carboxylates tried over a number of years, however, failed in this type of side-chain derivatization. Yet, once suitable ligands have been identified, it is our experience that the process of side-chain derivatization of immodulin peptides is both reproducible and scalable. Table 4 shows the sequences of the successfully derivatized immodulin (SCDI) peptides used in this study.

3.4. Mechanistic specificity

Figure 2 shows the mechanistic specificities conferred by each of eight different nuclear receptor ligand side-chains (FXR, PPAR α , PPAR γ , RAR α , RAR α/β , RAR γ , RAR β/γ , RXR) when tested in four cell types of skin tissue. The panels, from top to bottom, show: (a) the effects of RAR α/β -modified peptides on CD169+ differentiation

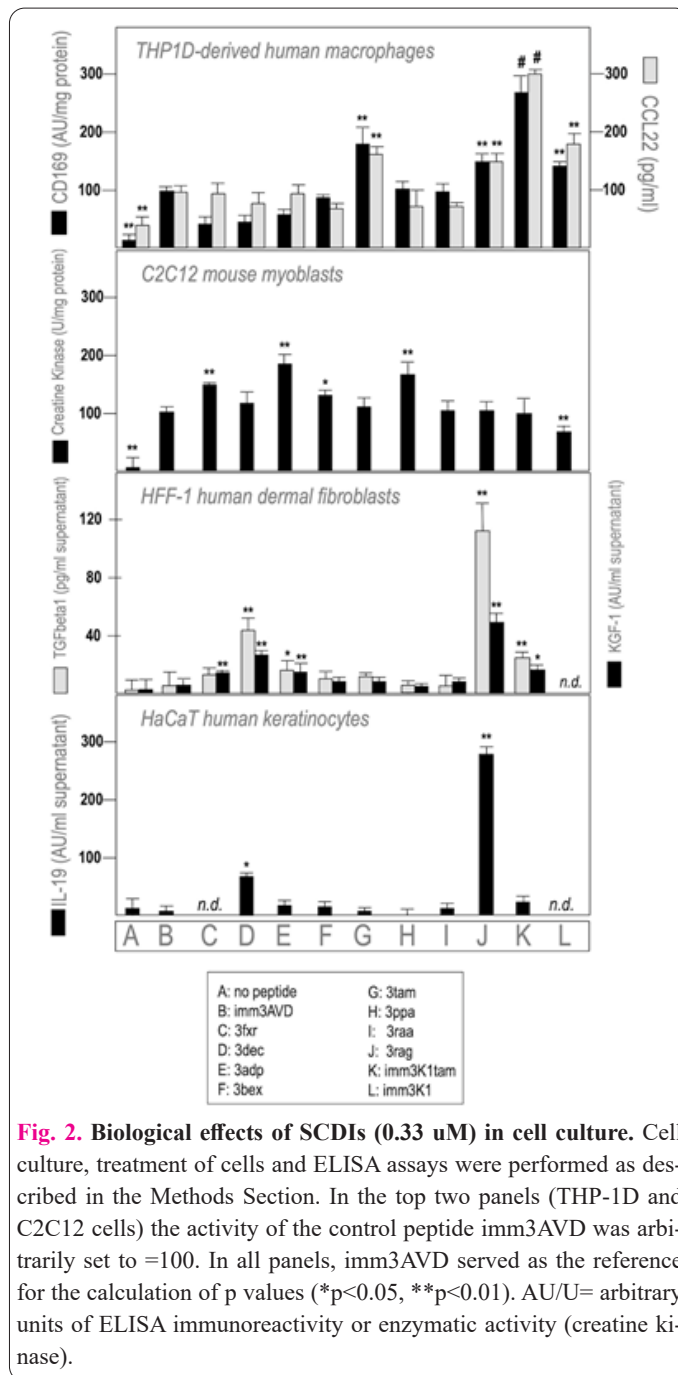


Fig. 2. Biological effects of SCDIs (0.33 μ M) in cell culture. Cell culture, treatment of cells and ELISA assays were performed as described in the Methods Section. In the top two panels (THP-1D and C2C12 cells) the activity of the control peptide imm3AVD was arbitrarily set to =100. In all panels, imm3AVD served as the reference for the calculation of p values (* p <0.05, ** p <0.01). AU/U= arbitrary units of ELISA immunoreactivity or enzymatic activity (creatine kinase).

Table 4. Derivatized immodulin peptides (SCDI) and control peptides.

Peptide ID	Peptide sequence (*ligand conjugated at C-terminal lysine)	*C-terminal Ligand
imm3	KKGFYKKKQCRPSKGRKRGFCW	No ligand
imm3AVD	KKGFYKKKQCRPSKGRKRGFCWAVD	No ligand
imm3SVD	KKGFYKKKQCRPSKGRKRGFCWSVD	No ligand
imm3K1	SLNPEWNETKKGFYKKKQCRPSKGRKRGFCWAVD	No ligand
3ppa	SDKKGFYKKKQCRPSKGRKRGFCWSVDK*	PPAR α
3dec	SDKKGFYKKKQCRPSKGRKRGFCWSVDK*	PPAR γ
3fxr	SDKKGFYKKKQCRPSKGRKRGFCWSVDK*	FXR
3adp	SDKKGFYKKKQCRPSKGRKRGFCWSVDK*	RAR β/γ
3tam	SDKKGFYKKKQCRPSKGRKRGFCWAVDK*	RAR α/β
3rag	SDKKGFYKKKQCRPSKGRKRGFCWSVDK*	RAR γ
3raa	SDKKGFYKKKQCRPSKGRKRGFCWSVDK*	RAR α
3bex	SDKKGFYKKKQCRPSKGRKRGFCWSVDK*	RXR
imm3K1tam	SLNPEWNETDKKGFYKKKQCRPSKGRKRGFCWAVDK*	RAR α/β
3decK9adp	[PPAR γ]-SAFNSEYELGSDKKGFYKKKQCRPSKGRKRGFCWSVDK*	RAR β/γ
V-nephrilin	[valproic acid]-RGVTEDYLRLETLVQKVVSCKGFYKKKQCRPSKGRKRGFCW	

of unpolarized, THP-1D-derived human macrophages; (b) the effects of FXR-, PPAR α - and RXR-modified peptides on the differentiation of C2C12 mouse myoblasts into myotubes. It is worth noting that during wound healing skin fibroblasts differentiate into myofibroblasts and form myotubes [12,18,23]; (c) the effects PPAR γ - and RAR γ -modified peptides on TGF β 1 and FGF7/KGF-1 synthesis in human HFF-1 dermal fibroblasts and on IL-19, IL-22 and IL-24 secretion in TNF α /IFN γ -stimulated HaCaT human keratinocytes. Fibroblast FGF7 and keratinocyte IL-19 are believed to comprise part of a paracrine circuit in wound healing [11-15,18,25]. No peptide tested on a cell type in this study significantly affected the viability of any of the other cell types. In essence, these data point to a possible reservoir of SCDI-driven bioactivity that could, in theory, generate specific biological effects on target cells in skin tissue without toxicity to other cell types in their vicinity.

3.5. Features of SCDI-driven bioactivity and formulations

IL-20 family cytokines have been implicated in various aspects of wound healing [11-15,18,25]. We asked whether different designs of SCDIs might influence different parts of this biological process. Figure 3a shows that IL-19 and IL-24 are stimulated by RAR-modulating ligands bound to peptide, whereas IL-22, which is thought to modulate myofibroblast differentiation, is strikingly amplified by peptide 3dec, which is covalently modified with a partial PPAR γ agonist. A control experiment in the C2C12 assay system (Figure 3b) serves to illustrate the following points: the amplification of bioactivity mediated by SCDIs cannot be replicated at the same concentrations when peptide and ligand are added together but are not covalently bound. Ligand alone, at the same concentration, results in even lower bioactivity than the peptide control, presumably because the natural peptide sequence has low but detectable activity in this assay.

We next asked if unique SCDI-driven bioactivities could be amplified by PKC inhibition. Figure 3d shows that short, previously described, PKC-isoform-specific kinase inhibiting peptide sequences [19,20] can selectively amplify CD169⁺ macrophage differentiation from human THP-1D precursors and collagen synthesis by HFF-1 human dermal fibroblasts. Bioactivity *in vivo* can also be extended by formulations. Figure 3c shows how release of immodulin peptide from peptide-PLGA microparticles can be tripled by co-packaging the peptide with one of its natural ligands, transferrin [1,21]. In a rat burn-endotoxemia model [16] the addition of another natural ligand, hyaluronic acid [1], reduces breathing distress. Plasma albumin and body weight are also positively affected by using hyaluronic acid as an excipient in the same experiment (Figure 3e). Hyaluronic acid may function here by helping partition peptides into the lymphatic system [17].

3.6. Combinatorial SCDI diversity

The above results suggest that combinatorial diversity generated by derivatizing multiple side-chains on the same immodulin peptide can amplify and fine-tune mechanistic specificity. Notably, extending the peptide sequence to include PKC kinase isoform-inhibiting sequences [19,20] can further amplify some of these characteristics. We set out to combine these SCDI design elements to enhance

objectives such as macrophage differentiation or fibroblast collagen synthesis, as a demonstration of the combinatorial power of this platform.

Figure 4A shows the stepwise improvement by design of macrophage-differentiation activity achieved by combining SCDI with a C-terminal RAR α/β ligand and a PKC β kinase inhibitor peptide extension to form the imm3K-1tam peptide. Differentiation of CD169⁺ macrophages that secrete CCL22 and IL-10 is increased step-wise by these changes. In a mixed culture assay wherein CD169⁺ macrophages drive the polarization of naïve CD4⁺ T-helper cells in an overlay (Figure 4B), these design changes also increase the elaboration of FoxP3⁺ iTregs while significantly decreasing Th17 cells (IL-17).

In another example shown in Figure 4 (bottom panel), peptide 3decK9adp combines a C-terminal lysine side-chain derivatization (RAR β/γ ligand) with an N-terminal derivatization (PPAR γ ligand) and a peptide extension designed to enhance collagen synthesis in HFF-1 dermal fibroblasts. The results show stepwise increases in collagen production with addition of each design element.

Appropriate collagen synthesis by fibroblasts in wound

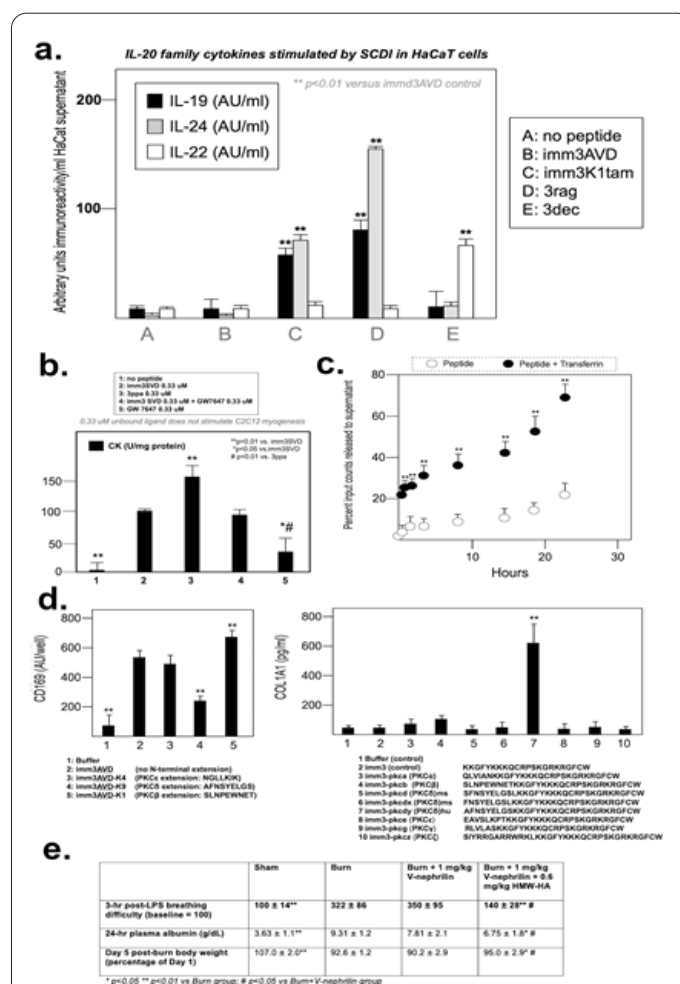
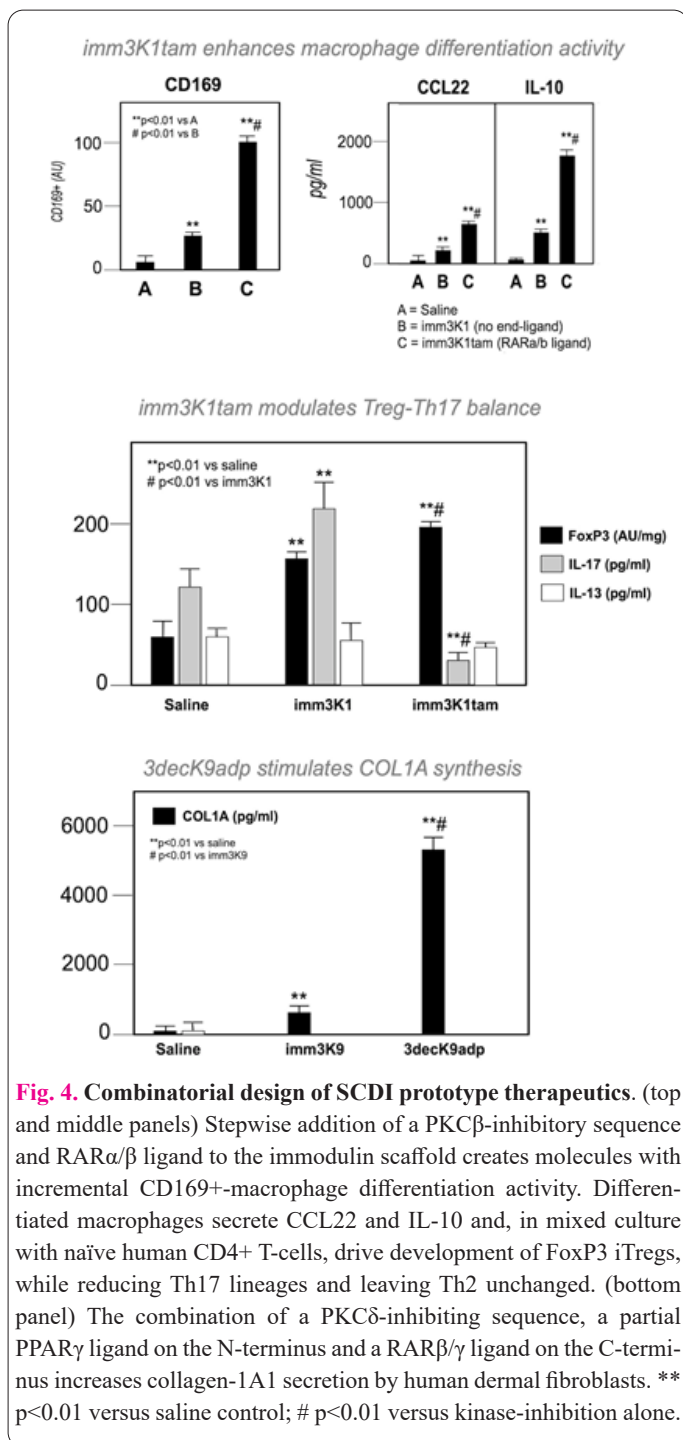


Fig. 3. Features of SCDIs and formulations. (A) IL-20 family cytokines induced by various SCDIs in HaCaT human keratinocytes. (B) Comparison of bound and unbound ligands in C2C12 assay. (C) The effect of holotransferrin on the release kinetics of peptide from PLGA microparticles. ** $p < 0.01$ versus peptide microparticles without holotransferrin. (D) The amplifying effects of kinase-inhibitory sequences. CD169 immunoreactivity (AU=arbitrary units of immunoreactivity) by ELISA; ** $p < 0.01$ versus imm3AVD control. (E) The effect of co-administered hyaluronic acid on the efficacy of V-nephhrilin peptide in the rat scald-endotoxemia model (see Methods).



healing and excessive synthesis of collagen in keloid scars and organ fibrosis are important phenomena in matrix biology. These results, taken together, provide a striking illustration of how transcriptional modulation of skin cells — in this case, fibroblasts — can have direct and immediate impacts on tissue matrix.

4. Discussion

A novel technological approach for transcriptional modulation of skin cell function with predicted effects on surrounding matrix is described in this work. The immodulin peptide scaffold used here provides the biological intelligence to target small-molecule epigenetic modulators (especially NR ligands for RXR-heterodimer partners such as PPARs and RARs) to the nuclei of targeted cells. At the nanomolar concentrations seen to be effective in our work such transcriptional effects cannot be easily duplicated using free ligands *in vivo*. Moreover, covalent at-

tachment to immodulins in SCDIs allows multiple ligands to be tested at equimolar concentrations within the same nucleus. The rationale for combining ligands is expansion of the combinatorial variance for tuning transcriptional effects in targeted cell types, thereby potentially expanding the power of the platform. An opportunity for the use of computational tools to accelerate the design process using combinatorial approaches in this context also bears mention.

When administered transdermally, SCDIs efficiently partition to surface tissues (skin and draining lymphatics) enriching relative local concentrations of peptide by nearly an order of magnitude when compared to plasma and major abdominal organs. Because of the peptides' unusual partitioning to skin *in vivo*, low nanomolar concentrations of SCDIs in plasma — two to three orders of magnitude lower than C_{max} in plasma for most traditional drugs — the concentrations believed to be sufficient for biological efficacy in skin cells, based on our cell culture studies, may provide an attractive safety profile for projected therapeutic uses. This apparently natural partitioning of immodulins, and the resulting anatomic specificity of their predicted therapeutic action in the form of SCDIs, may collaborate to generate highly desirable therapeutic indexes for this peptide class, especially in the context of “distance medicine”.

Mechanistically, the possibility of fine-tuning transcriptional programs in each of the major cell types within a targeted anatomical compartment by design, and establishing these specificities at low development cost from the outset, provides novel opportunities for next-generation therapeutic design. Recent studies of rapidly changing patient preferences [10] and the steady evolution of vertically integrated healthcare delivery systems towards “distance medicine” suggest an emerging premium on high-safety, self-administered drug modalities.

Using the SCDI platform, we have provided several examples of tunable transcriptional events in cultured human skin cells. In this approach, the immodulin peptide scaffold (a natural RXR adaptor [1]) is covalently linked to one or more small-molecule ligands of RXR-heterodimers such as PPARs and RARs and then screened for biological effects in human skin cell culture. We have provided examples using unpolarized macrophages, dermal fibroblasts, keratinocytes and myoblasts showing, for the first time, that (a) a RAR α/β ligand can drive CD169 $^{+}$ macrophage differentiation, with implications for local tissue-specific antigen tolerization via iTregs [1]; (b) an RAR γ agonist and a partial PPAR γ ligand can stimulate IL-19, IL-22 and IL-24 production from HaCaT human keratinocytes and FGF7/KGF-1 and TGF β production from human HFF-1 dermal fibroblasts, these cytokines representing known components of a paracrine circuit important to healing tissue [11-15,18,25]; and (c) a PPAR α ligand can stimulate myogenesis, a process potentially relevant to myofibroblast differentiation and strength of tissue in late skin healing. To our knowledge, such diversity of purposeful transcriptional redirection in adjacent skin cell types, each event driven by a unique side-chain modification of a natural peptide sequence, has never been demonstrated.

The use of immodulins as scaffolds for epigenetic therapeutics has been attempted for over a decade. In numerous rodent models, modified immodulins have been successfully shown to reduce metabolic, xenobiotic and

traumatic stresses [24], notably in a rat scald model [16]. Recently, underlying mechanisms of action for this family of peptides have been elucidated. Immodulins function by rapidly entering cells and altering their transcriptional activity, binding directly to RXR α and RXR γ isoforms and to heterodimeric partners such as Nur77 and PPAR α [1]. The current study demonstrates, for the first time, another previously unknown feature of immodulin action: global anatomical partitioning of peptides to peripheral tissues when administered through the skin, regardless of the limb where transdermal administration occurs. Moreover, the feasibility of repurposing previously characterized nuclear receptor molecules as covalent attachments to lysine side-chains of immodulin peptides — albeit in that modified form — opens up the possibility of marrying a rich chemical diversity of traditional small-molecule drugs with the targeting intelligence of immodulin peptides. For example, our current understanding of the sequence of cellular events in wound healing [11-15,18,25] can lead to precise hypothesis testing in wound-healing rodent models using peptides described in this work.

Many elegant technologies have failed in the real world for unforeseen reasons and we appreciate the fact that SCDI technology awaits validation in rodent models and human disease. Many inflammatory conditions of the skin, as well as healing and regeneration of tissues, would seem to represent obvious targets for future testing. The prior success of earlier designs within this class of peptides as therapeutics in the rat burn model raises hopes for future progress using SCDIs [16].

Several drawbacks to this study should be noted. First, we did not test intradermal injection of peptides as an alternative to the transdermal route we explored in this study. We intend to address this issue in a future study. Second, as outlined above, the success rate in constructing SCDIs is limited by the cost of ligand synthesis, the limitation of requiring a single free carboxyl group in the structure of the ligand, patent considerations and low chemical conjugation yields for some ligands (for reasons that are, as yet, unclear even after several years of research). Third, although the theoretical argument suggests a rationale for why SCDIs may provide lower effective doses and minimal toxicity, this proposition awaits confirmation in actual GLP safety studies. The cost of such studies is substantial, but such studies will need to be performed before safety claims for the class can be fully supported. The changing landscape of funding for preclinical biotechnology research is perhaps the greatest challenge that limits progress on new drug development technologies prior to their validation in the clinic. Lastly, global analysis of transcriptional repertoires in target tissues such as skin would help us confirm the expectation of mechanistic specificity of SCDIs, an expectation currently derived from assaying selected analytes, as in the cell culture studies reported here. We intend to initiate those molecular studies in the near future. Our focus is to achieve a better understanding of how temporal specificity of release can help sequence and synchronize the effects of SCDIs with natural transcriptional patterns in skin, such as during wound healing.

A novel technological approach for using SCDIs to modulate biological events in skin cells is described in this work. The immodulin peptide scaffold used here potentially provides the biological intelligence to target small-molecule epigenetic modulators (especially NR ligands

for RXR-heterodimer partners such as PPARs and RARs) to the nuclei of targeted cells, creating highly precise therapeutic possibilities. Pressure from patients and regulators has set an ever-rising bar with respect to the safety of future drugs. Anatomical and mechanistic specificity of therapeutic molecules is required for such a reduction in off-target effects. In this work, we explore the use of a “biologically intelligent” skin-homing peptide (immodulin peptide) which can rapidly enter a cell’s nucleus and bind RXR, a master transcription factor in mammalian cells. By chemically modifying immodulins with small-molecule RXR heterodimer ligands known to alter relevant subsets of RXR-driven transcriptional programs, we identify transcriptional modulators that may modulate processes known to drive the resolution of inflammation and healing of human skin tissue via the concerted action of monocytes, keratinocytes and fibroblasts.

Abbreviations

NR: nuclear receptor; RXR: retinoid X receptor; SCDI: side-chain derivatized immodulin; iTregs: induced Tregs; RAR α/β : retinoic acid receptor α/β ; IL-19: interleukin-19; KGF-1: keratinocyte growth factor-1; TGF β : transforming growth factor- β ; COL1A1: collagen 1A1; RAR γ : retinoic acid receptor- γ ; PPAR γ : peroxisome proliferator-activated receptor- γ .

Conflicts of interest

All authors except D.D.M declare no conflicts of interest. D.D.M states he has filed patent applications relating to this work. None of the four institutions own any patents or patent applications related to this work. D.D.M. is the founder and owns shares in Transporin Inc., which does not sell products or receive commercial revenue. D.D.M. does not receive a salary, stipend or consulting fee from any corporation or commercial entity.

Consent for publication and ethics declaration

All authors have read and approved the final manuscript for publication. We confirm that neither the manuscript nor any parts of its content are currently under consideration for publication with or published in another journal. The animal study protocol was approved by the Institutional Review Board of the Molecular Medicine Research Institute. All animal studies complied with the NIH Guide for the Care and Use of Laboratory Animals.

Availability of data and material

The authors declare that they embedded all data in the manuscript.

Author contributions

Conceptualization, D.D.M. and D.P.; methodology, D.D.M. and D.P.; formal analysis, D.D.M.; investigation, D.D.M., B.P., P.R., A.B.; resources, D.D.M. and E.A.; writing—original draft, D.D.M.; writing—review and editing, D.D.M., B.P., E.A.; project administration, D.D.M.; funding acquisition, D.D.M. All authors have read and agreed to the published version of the manuscript.

Funding

This study was supported by the Mayflower Research Institute, a 501c3 non-profit funded by charitable contributions. No specific funding was received for this project.

References

1. Mascarenhas DD (2022) Immodulin peptides influence musculoskeletal homeostasis by linking extracellular cues to macrophage and myoblast nuclear receptors. *Eur J Transl Myol* 32:10695. doi: 10.4081/ejtm.2022.10695
2. Baxter RC (2015) Nuclear actions of insulin-like growth factor binding protein-3. *Gene* 569:7-13. doi:10.1016/j.gene.2015.06.028
3. Boehm MF, Zhang L, Zhi L, McClurg MR, Berger E, Wagoner M, Mais DE, Suto CM, Davies JA, Heyman RA (1995) Design and synthesis of potent retinoid X receptor selective ligands that induce apoptosis in leukemia cells. *J Med Chem* 38:3146-55. doi: 10.1021/jm00016a018
4. Bookout AL, Jeong Y, Downes M, Yu RT, Evans RM, Mangelsdorf DJ (2006) Anatomical profiling of nuclear receptor expression reveals a hierarchical transcriptional network. *Cell* 126:789-99. doi: 10.1016/j.cell.2006.06.049
5. Brown PJ, Stuart LW, Hurley KP, Lewis MC, Winegar DA, Wilson JG, Wilkison WO, Ittoop OR, Willson TM (2001) Identification of a subtype selective human PPARalpha agonist through parallel-array synthesis. *Bioorg Med Chem Lett* 11:1225-7. doi: 10.1016/s0960-894x(01)00188-3
6. Dominguez M, Alvarez S, de Lera AR (2017) Natural and Structure-based RXR Ligand Scaffolds and Their Functions. *Curr Top Med Chem* 17:631-662. doi: 10.2174/1568026616666160617072521
7. Huq, A., B. Singh, T. Meeker, and D. Mascarenhas (2009) The metal-binding domain of IGFBP-3 selectively delivers therapeutic molecules into cancer cells. *Anticancer Drug* 20:21-31. doi: 10.1097/CAD.0b013e3283144610
8. Singh, B., D. Charkowicz, and D. Mascarenhas (2004) Insulin-like growth factor-independent effects mediated by a C-terminal metal-binding domain of insulin-like growth factor binding protein-3. *J Biol Chem* 279:477-487. doi: 10.1074/jbc.M307322200
9. Koizumi H, Sato KC, Ohkawara A (1992) Effects of novel synthesized retinobenzoic acid (Am-80) on adenylate cyclase and arachidonic acid release in pig epidermis. *J Dermatol Sci* 3:97-102. doi: 10.1016/0923-1811(92)90042-a
10. Tetteh EK, Morris S, Titcheneker-Hooker, N. (2017) Discrete-choice modelling of patient preferences for modes of drug administration. *Health Economics Rev* 7:1-14. doi: 10.1186/s13561-017-0162-6
11. Liu S, Hur YH, Cai X, Cong Q, Yang Y, Xu C, Bilate AM, Gonzales KAU, Parigi SM, Cowley CJ, Hurwitz B, Luo JD, Tseng T, Gur-Cohen S, Sribour M, Omelchenko T, Levorse J, Pasolli HA, Thompson CB, Mucida D, Fuchs E (2023) A tissue injury sensing and repair pathway distinct from host pathogen defense. *Cell* 186:2127-2143.e22. doi: 10.1016/j.cell.2023.03.031
12. Malapaka RRV, Khoo S, Zhang J, Choi JH, Zhou XE, Xu Y, Gong Y, Li J, Yong EL, Chalmers MJ, Chang L, Resau JH, Griffin PR, Chen YE, Xu HE (2012) Identification and mechanism of 10-carbon fatty acid as modulating ligand of peroxisome proliferator-activated receptors. *J Biol Chem* 287:183-195. doi: 10.1074/jbc.M111.294785
13. Werner S, Krieg T, Smola H (2007) Keratinocyte-fibroblast interactions in wound healing. *J Invest Dermatol* 127:998-1008. doi: 10.1038/sj.jid.5700786
14. Marti GP, Mohebi P, Liu L, Wang J, Miyashita T, Harmon JW (2008) KGF-1 for wound healing in animal models. *Methods Mol Biol* 423:383-91. doi: 10.1007/978-1-59745-194-9_30
15. Luo H, Wang Y, Su Y, Liu D, Xiao H, Wu M, Zhao Y, Xue F (2022) Paracrine effects of adipose-derived stem cells in cutaneous wound healing in streptozotocin-induced diabetic rats. *J Wound Care* 31(Sup3):S29-S38. doi: 10.12968/jowc.2022.31.Sup3.S29
16. Mascarenhas DD, Ravikumar P, Amento EP (2022) N-modulin peptides attenuate respiratory distress in a scald-endotoxemia model. *Burns Open* 6:1-6. doi.org/10.1016/j.burnso.2021.09.001
17. Fraser JR, Appelgren LE, Laurent TC (1983) Tissue uptake of circulating hyaluronic acid. A whole body autoradiographic study. *Cell Tissue Res* 233:285-93. doi: 10.1007/BF00238296
18. McGee HM, Schmidt BA, Booth CJ, Yancopoulos GD, Valenzuela DM, Murphy AJ, Stevens S, Flavell RA, Horsley V (2013) IL-22 promotes fibroblast-mediated wound repair in the skin. *J Invest Dermatol* 133:1321-9. doi: 10.1038/jid.2012.463
19. Ron D, Luo J, Mochly-Rosen D (1995) C2 region-derived peptides inhibit translocation and function of beta protein kinase C in vivo. *J Biol Chem* Oct 13;270:24180-7. doi: 10.1074/jbc.270.41.24180
20. Schechtman D, Mochly-Rosen D (2002) Isozyme-specific inhibitors and activators of protein kinase C. *Methods Enzymol* 345:470-89. doi: 10.1016/s0076-6879(02)45039-2
21. Weinzimer SA, Gibson TB, Collett-Solberg PF, Khare A, Liu B, Cohen P (2001) Transferrin is an insulin-like growth factor-binding protein-3 binding protein. *J Clin Endocrinol Metab* 86:1806-13. doi: 10.1210/jcem.86.4.7380
22. Shirakawa T, Miyawaki A, Matsubara T, Okumura N, Okamoto H, Nakai N, Rojasawasthien T, Morikawa K, Inoue A, Goto A, Washio A, Tsujisawa T, Kawamoto T, Kokabu S (2020) Daily Oral Administration of Protease-Treated Royal Jelly Protects Against Denervation-Induced Skeletal Muscle Atrophy. *Nutrients* 12:3089. doi: 10.3390/nu12103089
23. Schuster R, Younesi F, Ezzo M, Hinz B (2023) The Role of Myofibroblasts in Physiological and Pathological Tissue Repair. *Cold Spring Harb Perspect Biol* 15(1):a041231. doi: 10.1101/cshperspect.a041231
24. Singh BK, Singh A, Mascarenhas DD (2010) A nuclear complex of rictor and insulin receptor substrate-2 is associated with albuminuria in diabetic mice. *Metab Syndr Relat Disord* 8:355-63. doi: 10.1089/met.2010.0011
25. Sun DP, Yeh CH, So E, Wang LY, Wei TS, Chang MS, Hsing CH (2013) Interleukin (IL)-19 promoted skin wound healing by increasing fibroblast keratinocyte growth factor expression. *Cytokine* 62:360-8. doi: 10.1016/j.cyto.2013.03.017